JOURNAL OF SOLID STATE CHEMISTRY 75, 105–112 (1988)

Crystal Growth and Electrical Properties of $CuFeO_2$ Single Crystals

P. DORDOR, J. P. CHAMINADE, A. WICHAINCHAI,*
E. MARQUESTAUT, J. P. DOUMERC, M. POUCHARD,
AND P. HAGENMULLER

Laboratoire de Chimie du Solide du CNRS, Université de Bordeaux I, 351, course de la Libération, 33405 Talence Cedex, France

AND A. AMMAR

Laboratoire de Chimie du Solide Minéral, Faculté des Sciences, Université Cadi-Ayyad, Marrakech, Maroc

Received October 6, 1987; in revised form January 18, 1988

Delafossite-type $CuFeO_2$ single crystals have been prepared by a flux method: crystals obtained in a Cu crucible with $LiBO_2$ as flux are *n*-type whereas those prepared in a Pt crucible with a Cu_2O flux are *p*-type. Electrical measurements have revealed that *n*-type crystals exhibit weak anisotropic conductivities with large activation energies and small mobilities (r.t. values perpendicular and parallel to the *c*-axis: $\mu_\perp = 5 \times 10^{-5}$ and $\mu_\parallel = 10^{-7}$ cm^{-2} V^{-1} sec^{-1}). *p*-type crystals, less anisotropic, are characterized by low activation energies and higher mobilities ($\mu_\perp = 34$ and $\mu_\parallel = 8.9$ cm^2 V^{-1} sec^{-1}). A two-conduction-band model is proposed to account for the difference observed between the energy gap value deduced from photoelectrochemical measurements and the activation energy of the electrical conductivity in the intrinsic domain. © 1988 Academic Press, Inc.

Introduction

Many studies have been devoted to $CuFeO_2$ which was historically the first known compound exhibiting the so-called delafossite structure. Such a structure consists of close packed oxygen double layers in which the octahedral sites are occupied by Fe^{3+} cations. These double layers are linked by monovalent Cu^+ ions with a two-fold oxygen linear coordination as shown in Fig. 1 (*1, 2*).

Magnetic properties have been intensively studied. $CuFeO_2$ is antiferromagnetic ($T_N = 13$ K) with stronger interactions within the layers than along the *c*-axis, as could be anticipated from the structure (*3*). Calculations of the lattice energy and Mössbauer spectroscopy measurements have confirmed the monovalent and trivalent oxidation states of copper and iron, respectively.

The opto-electronic and electrical properties of *p*- and *n*-type polycrystalline $CuFeO_2$ have been recently investigated, at room temperature, by Benko *et al.* (*4*). These authors have found that the carrier

* Permanent address: Applied Physics Department, Faculty of Sciences, King Mongkut Institute Technology, Lad-Kabang, Bangkok 10520, Thailand.

0022-4596/88 $3.00

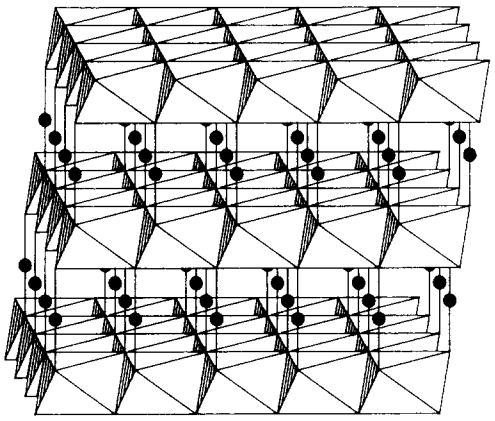

FIG. 1. Delafossite-type structure. Solid black circles represent the copper atoms.

mobility in *p*-type samples is much higher than that in *n*-type ones. They have attributed this behavior to two different conduction mechanisms involving Cu^+ and Fe^{3+}, respectively.

Despite the 2D-character of the structure only one paper reports measurements of the anisotropy of transport properties of $CuFeO_2$ single crystals (*5*).

Photoelectrochemical characterization and thermal variation of electrical properties of pure and Pt-doped single crystals reported here confirm the model of Benko *et al.* (*4*). Special attention is paid to the anisotropy and its variation with temperature.

Sample Preparation and Crystal Growth

$CuFeO_2$ polycrystalline samples have been prepared by solid state reaction between Cu_2O and Fe_2O_3 with the molar ratio 3 : 1 as previously described (*3*). Pellets were sintered at $T = 1325$ K for 48 hr in a silica tube sealed under vacuum and then quenched at room temperature.

The Cu-delafossite-type compounds melt incongruently so that a flux method has been chosen for the single crystal growth. Examination of the Cu–Fe–O phase diagram shows the possibility of growing crystals from a copper rich flux of mixed oxides in air (*6*). The starting oxides were CuO (Ultrapure from Alpha Ventron) and Fe_2O_3 (Specpure from Johnson Matthey). A mixture of thoroughly ground CuO and Fe_2O_3 powder (wt. $\simeq$ 20 g) was introduced into a 30-cm^3 platinum crucible and then heated in air. Starting composition, thermal cycle, and results are given in Table I.

Only small size single crystals, referred to as Cx(Pt), could be obtained. They were separated from solidified copper oxide by leaching using hot diluted nitric acid for 7 days. The platinum crucible was attacked by the mixture and traces of Pt have been detected in the crystals as shown below. The main problems encountered using those experimental conditions result from

(i) the high chemical reactivity of copper (I) oxide above 1300 K in the solid and particularly in the molten state ($T_M \simeq 1398$ K in air),

(ii) the strong influence of the oxygen partial pressure on the Cu_2O/CuO equilibrium (*7*).

The previous remarks led us to select a copper crucible and lithium metaborate as solvent. A mixture (wt. $\simeq$ 20 g) of $LiBO_2$ (Specpure), Cu_2O (99.95% from Alpha Ventron), and Fe_2O_3 (Specpure from Johnson Matthey) was introduced into the crucible and heated in an alumina reaction tube swept by a flow (2 liters/hr) of dried argon ($P_{O_2} \simeq 10^{-4}$ atm). Growth conditions are summarized in Table I.

Small single crystals, referred to as Cx(Cu), were easily recovered by washing with hot diluted nitric acid in an ultrasonic pot. In both cases the as-grown crystals were examined with an optical microscope in order to reject samples containing flux.

The chemical composition of crystals from both growth methods has been confirmed by electronic microprobe analysis. As already mentioned traces of Pt were detected in Cx(Pt) single crystals. The Pt concentration is approximately of 0.08 mole%

TABLE I

CRYSTAL GROWTH CONDITIONS

Ref.	Composition	Crucible	Atmosphere	Thermal cycle	Results
Cx(Pt)	4.5 CuO + $\frac{1}{2}$ Fe_2O_3	Pt	Air	Heating up to 1180°C at 50°C/hr 10-hr soak at 1180°C Cooling down to 1020°C at 2°C/hr Final cooling down to room temperature at 30°C/hr	Black hexagonal or triangular platelets with (001) principal faces and 2 × 2 × 0.3 mm^3 size
Cx(Cu)	0.04 Cu_2O + 0.04 Fe_2O_3 + 0.92 $LiBO_2$	Cu	Argon	Heating up to 950°C at 50°C/hr 10-hr soak at 950°C Cooling down to 820°C at 2°C/hr Final cooling down to room temperature at 30°C/hr	Black platelets with (001) principal faces and 3 × 3 × 0.1 mm^3 size

and homogeneously distributed in the crystal.

The lattice parameters were determined on ground crystals from X-ray powder diffraction data with Si as standard. The parameter values, listed in Table II, are in a good agreement with a hexagonal cell of delafossite-type structure but show some small fluctuations which could be attributed to a slight departure from stoichiometry. The $R\bar{3}m$ space group has been confirmed on Weissenberg photographs.

Experiments and Results

Electrical Conductivity

The electrical conductivity measurements on polycrystalline samples have been carried out using the four-colinear-probe method and automatic equipment described elsewhere (*8*). In order to give evidence of the anisotropy of conductivity in single crystals which are plate-like shaped with the main faces perpendicular to the *c*-axis, several methods have been used depending on the sample length in the current carrying direction. As the $\sigma_\perp$ conductivity measured in natural faces ($\perp$ to *c*-axis) is isotropic, no problem arises from the contact position and the four collinear probe method is quite convenient. For conductivity measurements performed along the *c*-axis ($\sigma_\parallel$) the contact position is more critical so that the Montgomery's method apparently seems more appropriate (*9*).

However, both methods were tried on Cx(Pt) single crystals which are relatively thick (≃0.3 mm) and a quantitative agreement has been found between experimental results. For Cx(Cu) single crystals the thickness of which is about 0.1 mm the previous methods fail and the original pattern described by Rogers *et al.* appears to be more suitable (*5*). Nevertheless its application is restricted by the condition $\sigma_\perp \gg \sigma_\parallel$

TABLE II

LATTICE PARAMETERS OF $CuFeO_2$

Ref.	*a*(Å)	*c*(Å)
Polycryst.	3.035 ± 0.001	17.16 ± 0.01
Cx(Pt)	3.030 ± 0.001	17.15 ± 0.01
Cx(Cu)	3.032 ± 0.001	17.15 ± 0.01

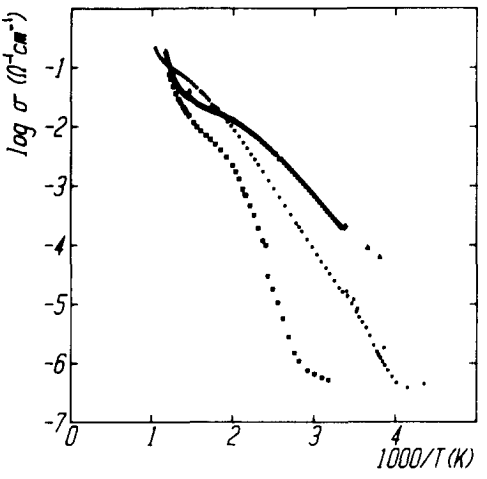

FIG. 2. Logarithm of electrical conductivity vs reciprocal temperature for $CuFeO_2$ single crystals [ref. Cx(Cu)]: (▲) ⊥ to the c-axis, (■) ∥ to the c-axis, and for (●) polycrystalline samples.

which has to be satisfied as the equipotential planes are assumed to be parallel with the layers. If this condition is not fulfilled the two-probe method leads to more significant results.

The variation of the conductivity vs reciprocal temperature of polycrystalline samples and of the Cx(Cu) single crystals are compared in Fig. 2.

For polycrystalline samples the conductivity follows an Arrhenius law in the 250–500 K temperature range, the corresponding activation energy being $\Delta E = 0.41$ eV. Between 500 and 750 K, $d(\log \sigma)/d(1/T)$ first decreases and then increases for higher temperatures, suggesting a transition from an extrinsic to an intrinsic-type behavior.

The electrical conductivity of Cx(Cu) single crystals has been measured from room temperature up to 850 K both parallely and perpendicularly to the c-axis (Fig. 2). The large anisotropy observed at $T = 300$ K ($\sigma_\perp/\sigma_\parallel \simeq 500$) decreases at increasing temperature. The behavior of $\sigma_\perp$ and $\sigma_\parallel$ vs $1/T$ gives evidence of temperature domains where the conductivities follow an Arrhenius law as observed before in the case of polycrystalline samples. Values of activation energy are given in Table III.

The electrical conductivity of Cx(Pt) single crystals has been measured in the 7–800 K temperature range as shown in Fig. 3.

TABLE III

ELECTRICAL PROPERTIES OF $CuFeO_2$ AT ROOM TEMPERATURE

Materials	Type	ΔE^σ (eV)	ΔE^α (eV)	A	n (or p)[a] (cm^{-3})	σ (Ω^{-1} cm^{-1})	μ (cm^2 V^{-1} sec^{-1})
Polycryst. (this work)	n	4.1×10^{-1}	0.13	3.4	1.2×10^{20}[b]	1.9×10^{-5}	1×10^{-6}
Polycryst. 1% Sn (*4*)	n	—	0.12	0	1.8×10^{19}[b]	3.2×10^{-5}	1.1×10^{-6}
Cx(Cu) (this work)	n	9.4×10^{-1}(∥) 2.8×10^{-1}(⊥)	0.17(∥) —	2.7	1.8×10^{10}[b]	6.5×10^{-7}(∥) 3.1×10^{-4}(⊥)	2.3×10^{-7}(∥) 1.1×10^{-4}(⊥)
Cx(Pt) (this work)	p	8.9×10^{-3}(∥) 9.3×10^{-3}(⊥)	— —	—	1.8×10^{19}[c]	25 (∥) 96 (⊥)	8.9 (∥) 34 (⊥)
Polycryst. (*4*)	p	—	0.17	—	3.9×10^{19}[b]	1.53	0.27
Cryst. (*5*)	—	2.3×10^{-1}(∥) 5×10^{-2}(⊥)	— —	—	—	3.3×10^{-4}(∥) 2 (⊥)	— —

[a] assuming one type of carriers,
[b] carrier number deduced from thermoelectric power measurements,
[c] carrier number deduced from Hall measurements;
∥ parallel to c-axis,
⊥ perpendicular to c-axis.

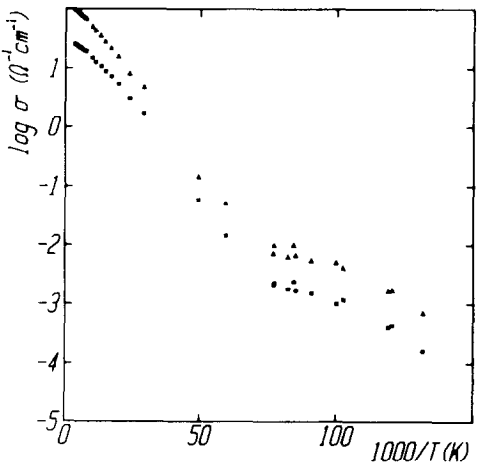

FIG. 3. Logarithm of conductivity vs reciprocal temperature for Pt-doped $CuFeO_2$ single crystals [ref. Cx(Pt)]: (▲) $\perp$ to the c-axis and (■) $\parallel$ to the c-axis.

The anisotropy determined by Montgomery's method is small ($\sigma_\perp/\sigma_\parallel \simeq 3.8$ at T = 300 K) and nearly independent of temperature. Between 30 and 300 K the variation of $\log(\sigma)$ vs $1000/T$ is linear. A departure from that behavior is observed near the Néel temperature (T_N = 13 K) (*3*). The activation energy values below and above T_N are given in Table III. From 300 to 420 K the conductivities are nearly constant and slightly decrease for higher temperatures.

Thermoelectric Power

The thermoelectric power α of polycrystalline samples has been measured from 160 to 1000 K. As shown in Fig. 4, α is negative in the investigated temperature range. The behavior of α vs $1000/T$ can be divided into two temperature ranges ($170 < T < 650$ and $T > 730$ K) corresponding to those observed for the conductivity variation. Inside those temperature domains $|\alpha|$ increases monotonically with reciprocal temperature. The activation energy of the thermoelectric power in the 160–300 K temperature range is much lower than that of the conductivity as shown in Table III.

For Cx(Cu) single crystals the very small thickness of the sample leads to a poor thermal contact between the sample and its holder when the thermal gradient is applied in the layer direction and consequently prevents one from making measurements in this direction. As a result, the thermoelectric power $\alpha_\parallel$ could only be determined with the thermal gradient parallel to the c-axis. Between 190 and 300 K, α is negative and its absolute value decreases at increasing temperature (Fig. 4). The activation energy deduced from the thermoelectric power is higher than that of polycrystalline samples as shown in Table III.

The thermoelectric power for Cx(Pt) single crystals could be measured from 10 to 300 K in both directions parallel and perpendicular to the c-axis. For $T > 25$ K the behavior of $\sigma_\parallel$ and $\sigma_\perp$ is similar: α is positive and increasing with temperature as shown in Fig. 5. Below 25 K, $\alpha_\parallel$ tends to zero while $\alpha_\perp$ abruptly decreases becoming even negative at $T \simeq 25$ K.

Photoelectrochemical Measurements

The photoelectrochemical measurements were carried out in a 0.1 M Na_2HPO_4 solu-

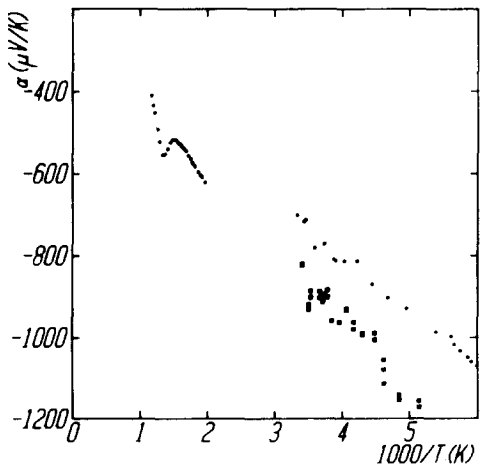

FIG. 4. Thermoelectric power vs reciprocal temperature for $CuFeO_2$ single crystals [ref. Cx(Cu)]: (■) $\parallel$ to the c-axis and (●) polycrystalline sample.

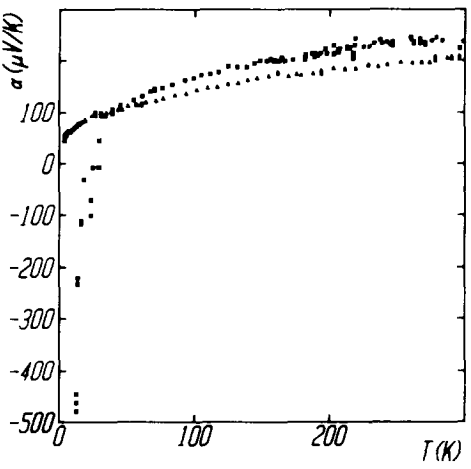

FIG. 5. Thermal variation of thermoelectric power of Pt-doped $CuFeO_2$ single crystals [ref. Cx(Pt)]: (▲) ⊥ to the c-axis, (■) ∥ to the c-axis.

tion (pH = 9.2) using an equipment described elsewhere (*10*). A natural face perpendicular to the c-axis of a p-type single crystal Cx(Pt) was used as the active surface of the electrode.

The quantity $(\eta h\nu)^{1/2}$ where η is the quantum efficiency is plotted vs photon energy $h\nu$ in Fig. 6. The linear variation observed between 1.29 and 3.10 eV shows that the transition corresponding to the band gap is indirect with E_g = 1.26 eV. This value is slightly higher than that determined by Benko and Koffyberg on a p-type $CuFeO_2$ polycrystalline sample (1.15 eV) (*4*). A more detailed study of the anisotropic behavior using polarized light with a face parallel to the c-axis as the surface electrode will be published elsewhere.

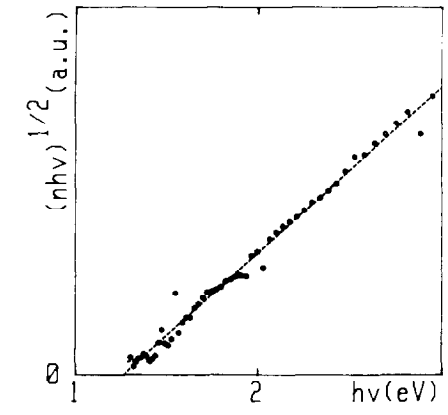

FIG. 6. Determination of the energy gap for $CuFeO_2$ single crystals [ref. Cx(Pt)].

Discussion

The electrical behavior of polycrystalline samples is relatively close to that of Cx(Cu) single crystals. In both cases the low electrical conductivity and negative thermoelectric power are thermally activated.

On the contrary, Cx(Pt) single crystals have a positive thermoelectric power increasing with temperature and their electrical conductivity is very weakly activated.

p-Type Samples

The simplest hypothesis for explaining the p-type semiconducting behavior is to attribute the acceptor levels to the platinum atoms detected by electronic microprobe analysis. That hypothesis is supported by Hall effect measurements which lead to a carrier concentration equal to the Pt concentration. Using the classical equation

$$\sigma = ne\mu \qquad (1)$$

one obtains the r.t. values of the mobility given in Table III. The difference in the mobility values (about one order of magnitude) between our results and those previously reported by Benko and Koffyberg, as shown in Table III, is not very surprising if we take into account

(i) the difference in the nature of the samples: single crystals (this work) or polycrystalline samples (*4*),

(ii) the difference in the doping elements and the sites they probably occupy: platinum in Cu^+-planes (this work) or magnesium in Fe^{3+}-planes (*4*), and

(iii) the determination methods of the number of carriers from Hall effect measurements in the present work and from thermoelectric power measurements in Ref. (*4*).

n-Type Samples

The observed *n*-type semiconducting behavior of "pure" $CuFeO_2$ could be ascribed to oxygen vacancies leading to the formation of donor levels. The formation of Cu^0 is very unlikely since no other Cu-delafossite compound exhibits a *n*-type semiconducting behavior. Therefore, donor levels are rather Fe^{2+} ions more or less trapped in the vicinity of oxygen vacancies.

For *n*-type semiconductors the thermoelectric power is given by

$$\alpha = -k/e(\Delta E_F/kT + A) = -k/e(\ln N_0/n + A), \quad (2)$$

where N_0 is the effective density of states in the conduction band, n is the carrier density, and the other quantities have their usual meaning. Assuming that the iron 3*d*-band is sufficiently narrow so that the corresponding energy levels are degenerated, N_0 has the same order of magnitude as the density of iron atoms, i.e., $N_0 \simeq 2.2 \times 10^{22}$ cm^{-3}.

The mobility values derived from Eqs. (1) and (2) are given in Table III. They are in agreement with that reported by Benko and Koffyberg for a *n*-type 1% Sn-doped sample (Table III). Such low mobility values are characteristic of a hopping conduction mechanism. Therefore electrical transport near room temperature is likely due to electrons thermally excited into the Fe^{3+} : 3*d* narrow band resulting from the t_{2g}^{β}-orbitals. This interpretation is in agreement with the very strong anisotropy observed in that temperature range: t_{2g}^{β}-orbitals are rather nonbonding and therefore a direct overlapping is only possible in planes perpendicular to the *c*-axis. We shall see below that covalent bonding between 4*s* (iron) and 2*p* (oxygen) orbitals apparently decreases the anisotropy to a large extent.

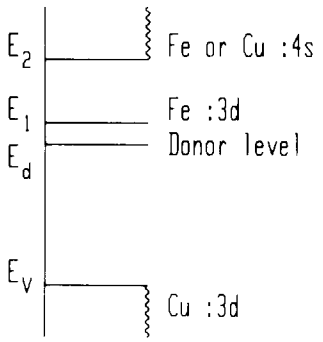

FIG. 7. Schematic energy diagram proposed for *n*-type $CuFeO_2$.

When temperature is raised, an intrinsic behavior seems to be reached (Fig. 2). However, the activation energy of the conductivity ($\Delta E^{\sigma} = 0.9$ eV) is much higher than the value expected from photoelectrochemical measurements, i.e., $E_g/2 = 0.6$ eV. Such a behavior can be understood only if we consider the electrical transport at high temperature to be governed by carriers excited into a conduction band of higher energy (E_2) where the mobility (μ_2) exceeds much of that of the lowest conduction band (μ_1). The corresponding energy diagram is schematized in Fig. 7.

From r.t. measurements Benko and Koffyberg have proposed that the conduction band (corresponding to the band of energy E_1 in Fig. 7) and the valence band result from the 3*d*-levels of iron and copper, respectively. Their interpretation is based on the difference of mobility values between *n*- and *p*-type samples (*4*). The present results confirm such a mobility difference (Table III) which can be explained by the following considerations:

—a very low mobility (μ_1) corresponding to a hopping-type transport is expected for the electrons occupying the 3*d*-orbitals

of Fe^{3+} which have a rather localized character,

—the much higher mobility (μ_v) of carriers in the copper $3d$-levels ($\mu_v > 10^5\mu_1$ as quoted in Table III) can result from a relatively large overlapping of hybridized $3d_z2$-$4s$ orbitals.[1]

On the other hand the negative sign of thermoelectric power shows that the investigated temperature range μ_2 should be larger than μ_v. In such conditions the band at energy E_2 could be identified simply with the $4s$-band either of iron or copper. Then the strong covalent character of the Fe–O or Cu–O bonds which are due to overlapping of the $4s$-orbitals (more or less hybridized with $4p$ and $3d$ levels) with the O : $2p$-orbitals could explain why the anisotropy tends to disappear at high temperature.

[1] For a more detailed discussion see Ref. (*5*) where Rogers *et al.* show that the stabilization of the two-fold coordination of d^{10} cations is associated with a $3d_z2$-$4s$ hybridization, the resulting orbitals having their electrostatic charge spread out in the copper plane.

It may also be mentioned that Cu–Cu distances are close to the critical r_c distance for localized vs delocalized states transition according to Goodenough (*10*) (neglecting the d_z2-$4s$ hybridization).

Acknowledgments

The authors are grateful to Dr. Lahaye for his contribution in EMA and to P. Keou for assistance in Hall effect measurements.

References

1. C. T. Prewitt, R. D. Shannon, and D. B. Rogers, *Inorg. Chem.* **10,** 719 (1971).
2. J. P. Doumerc, A. Ammar, A. Wichainchai, M. Pouchard, and P. Hagenmuller, *J. Phys. Chem. Solids* **48,** 37 (1987).
3. J. P. Doumerc, A. Wichainchai, A. Ammar, M. Pouchard, and P. Hagenmuller, *Mat. Res. Bull.* **21,** 745 (1986).
4. F. A. Benko and F. P. Koffyberg, *J. Phys. Chem. Solids* **48,** 431 (1987).
5. D. B. Rogers, R. D. Shannon, C. T. Prewitt, and J. L. Gillson, *Inorg. Chem.* **10,** 723 (1971).
6. D. S. Buist, A. M. M. Gadalla, and J. White, *Mineral. Mag.* **35,** 732 (1966).
7. R. D. Schmidt-Whitley, M. Martinez-Clemente, and A. Revcolevschi, *J. Cryst. Growth* **23,** 113 (1974).
8. P. Dordor, E. Marquestaut, C. Salduci, and P. Hagenmuller, *Rev. Phys. Appl.* **20,** 795 (1985).
9. H. C. Montgomery, *J. Appl. Phys.* **42,** 2971 (1971).
10. A. Ammar, A. Wichainchai, J. P. Doumerc, and M. Pouchard, *C.R. Acad. Sci. Paris* **303,** 353 (1986).